A TRIDENT SCHOLAR PROJECT REPORT

NO. 170

Development of an External Beam Ion Milliprobe

UNITED STATES NAVAL ACADEMY
ANNAPOLIS, MARYLAND

UNCLASSIFIED

SECURITY CLASSIFICATION OF THIS PAGE *(When Data Entered)*

REPORT DOCUMENTATION PAGE		READ INSTRUCTIONS BEFORE COMPLETING FORM
1. REPORT NUMBER U.S.N.A. - TSPR; 170 (1990)	2. GOVT ACCESSION NO.	3. RECIPIENT'S CATALOG NUMBER
4. TITLE *(and Subtitle)* DEVELOPMENT OF AN EXTERNAL BEAM ION MILLIPROBE.		5. TYPE OF REPORT & PERIOD COVERED Final 1989/90
		6. PERFORMING ORG. REPORT NUMBER
7. AUTHOR(s) Stephan A. MacLaren		8. CONTRACT OR GRANT NUMBER(s)
9. PERFORMING ORGANIZATION NAME AND ADDRESS United States Naval Academy, Annapolis.		10. PROGRAM ELEMENT, PROJECT, TASK AREA & WORK UNIT NUMBERS
11. CONTROLLING OFFICE NAME AND ADDRESS United States Naval Academy, Annapolis.		12. REPORT DATE 22 May 1990
		13. NUMBER OF PAGES 50
14. MONITORING AGENCY NAME & ADDRESS*(if different from Controlling Office)*		15. SECURITY CLASS. *(of this report)*
		15a. DECLASSIFICATION/DOWNGRADING SCHEDULE

16. DISTRIBUTION STATEMENT *(of this Report)*

This document has been approved for public release; its distribution is UNLIMITED.

17. DISTRIBUTION STATEMENT *(of the abstract entered in Block 20, if different from Report)*

18. SUPPLEMENTARY NOTES

Accepted by the U.S. Trident Scholar Committee.

19. KEY WORDS *(Continue on reverse side if necessary and identify by block number)*

Ion bombardment
Proton-induced X-ray emission

20. ABSTRACT *(Continue on reverse side if necessary and identify by block number)*

The goals of this Trident Project were the design, construction, testing, and initial application of an external beam ion milliprobe at the U.S. Naval Academy. The ion milliprobe is a tool for elemental analysis that employs the 1.7 million volt tandem electrostatic accelerator in Michelson C-7 to provide a beam of charged particles. The mechanism used for the analysis of elemental concentration is particle

(OVER)

DD FORM 1 JAN 73 1473 EDITION OF 1 NOV 65 IS OBSOLETE

S/N 0102-LF-014-6601

UNCLASSIFIED

SECURITY CLASSIFICATION OF THIS PAGE *(When Data Entered)*

induced x-ray emission (PIXE). This technique involves detecting and counting the x-rays produced when the focused beam of charged particles strikes the sample to be analyzed. This paper describes the design and construction of several essential specialized devices including an electrostatic quadrupole triplet lens, a current measuring collimator, an exit tip, and a sample enclosure. It discusses the procedures necessary to align, focus, and determine the size of the beam. Finally, the results of the initial analysis are evaluated and presented.

Development of an External Beam Ion Milliprobe

A Trident Scholar Project Report

by

Midshipman Stephan A. MacLaren, Class of 1990

U. S. Naval Academy

Annapolis, Maryland

Francis D. Correll

Associate Professor F. D. Correll
Physics Department

James R. Huddle

Assistant Professor J. R. Huddle
Physics Department

Accepted for Trident Scholar Committee

Dennis F. Hasson

Chairperson

22 May 1990

Date

USNA-1531-2

Abstract

The goals of this Trident Project were the design, construction, testing, and initial application of an external beam ion milliprobe at the U.S. Naval Academy. The ion milliprobe is a tool for elemental analysis that employs the 1.7 million volt tandem electrostatic accelerator in Michelson C-7 to provide a beam of charged particles. The mechanism used for the analysis of elemental concentration is particle induced x-ray emission (PIXE). This technique involves detecting and counting the x-rays produced when the focused beam of charged particles strikes the sample to be analyzed. This paper describes the design and construction of several essential specialized devices including an electrostatic quadrupole triplet lens, a current measuring collimator, an exit tip, and a sample enclosure. It discusses the procedures necessary to align, focus, and determine the size of the beam. Finally, the results of the initial analysis are evaluated and presented.

Acknowledgments

I would like to take the time to recognize and thank those individuals without whose help this project would not have been possible.

Mr. Charlie Holloway, the physics shop machinist, dedicated much time and effort to the careful preparation of mechanical parts for the milliprobe. Mr. Ken Zepp and Mr. Walt League assisted in the procurement of equipment and supplies in the physics lab decks. Mr. Ballman was especially helpful in providing parts from the EE department. Mr. Dale Campbell in the chemistry department supplied the chemicals necessary to create the shell standard and also demonstrated the use of the pellet press. Midshipman First Class Andrew H. Cook worked overtime with me second semester in order to accomplish the goals I had set. I extend my further appreciation to Assistant Professor Jeffery VanHoy for his knowledge of beamlines and his persistent effort in the laboratory. Paramount to the success of this project, however, was the assistance of my two advisors: Assistant Professor J. H. Huddle, who provided timely insight and continual help, especially in taking data, and Associate Professor F. D. Correll, whose supreme devotion of time, effort, wisdom, and foresight to the project deserves my utmost gratitude.

Thanks to Everyone,

Stephan A. MacLaren

Table of Contents

List of Figures

1. Introduction: Building a Tool for Elemental Analysis

"What is the composition of this sample?" Many branches of scientific research rely on a consistently accurate answer to this question. Therefore, the ability to analyze a sample in terms of the concentrations of its constituent elements is of great importance to scientists. In the past, elemental analysis has often been characterized by lengthy processes requiring chemical treatments that are not only time consuming but are usually destructive to the sample being tested.[1] In 1970, however, x-ray detectors were first used with low energy ion beams for the purpose of elemental analysis.[2] Now that low energy accelerators are available to many educational and research institutions, ion beam analysis has increased in popularity as opposed to other processes available. Ion beams offer a rapid, non-destructive, sensitive multi-elemental analytical method of determining concentrations.

1.1. Techniques of Elemental Analysis

Several different methods of elemental analysis using ion beams, or ion milliprobes, have been recently developed. These methods include ion beam nuclear activation (ACT), Rutherford backscattering (RBS), particle induced gamma ray emission (PIGE), and particle induced x-ray emission (PIXE).[3] An important feature of each of these methods is that they are essentially nondestructive.[4]

The PIXE technique, described in section 4.1, has been used in a wide variety of experimentation involving many diverse applications. These applications include investigations of impurity and wear in materials science[5], the determination of trace element distribution in mineralogical samples[6], analysis of suspended particles in urban river water[7], and even

analysis of the paper, parchment, and inks of historical documents for dating purposes.[8] This myriad of uses results from the major advantage of the PIXE method, its ability to acquire "fast and with minimal preparation, a determination of most of the chemical elements with a high and relatively uniform sensitivity and with convenient accuracy."[9]

An interesting specialization of the PIXE method is external beam analysis. This technique consists of allowing the bombarding protons to exit the vacuum of the accelerator beamline through a small opening covered by a thin foil. If the opening is sufficiently small and the foil material is sufficiently strong, it is possible to maintain a high vacuum in the beamline. External beam designs offer several important advantages. First, because the sample is not under a vacuum, it does not outgas due to trapped air or decomposition during beam irradiation; this would otherwise interfere with establishing a good vacuum in the beamline. Second, the air or other gas that surrounds the sample reduces sample damage by cooling and is also ionized by the beam so charge build-up does not take place. Finally, there is the inherent advantage of the simplicity of the design. Large and irregularly-shaped samples can be analyzed easily, as they do not have to fit inside a vacuum chamber, and positioning of the sample in front of the beam can be performed without an elaborate system of vacuum feed-through positioners.[10]

Taking into consideration the advantages listed above, an ion beam milliprobe is being developed for the U. S. Naval Academy. The milliprobe incorporates the external beam design into a setup for PIXE analysis. This program makes use of the Academy's new 1.7 million volt Pelletron tandem electrostatic accelerator in Michelson C-7.

1.2. The Ion Beam Milliprobe

"Milliprobe" is the term used to describe an ion beam that has been focused to a small size, typically fractions of a millimeter. An operational milliprobe requires more than just a beam of ions from an accelerator, however. It must be able to deliver a focused beam of particles to a specific point on a sample. This involves placing a small aperture in the beamline in order to create an optical "object" and focusing this object with a lens into an image on the target sample. In order for a beam of charged particles to travel any significant distance, they must be free from collisions with air molecules. Therefore, the accelerator and the entire beamline must be evacuated. Then, if the sample is to be placed outside the vacuum of the beamline, a method of extracting the beam from the vacuum chamber without destroying the integrity of the vacuum must be developed. An enclosure in which to mount and position the target must be built, and devices to detect, process and analyze the x-rays produced within the target must be positioned and interfaced. Finally, due to the potential hazards associated with an external beam, a system of safety shut-offs and interlocks must be installed.

1.3. Goals for the Project

The primary goal of this Trident project is to design and construct a fully operational external beam ion milliprobe. The milliprobe beamline as it exists in Michelson C-7 is illustrated by Figure 1. Once the various components are built and assembled, the detection and recording equipment is capable of handling data for a PIXE spectrum, and the accelerator is capable of safely delivering an ion beam to the milliprobe beamline, a series of tests must be performed. The diameter of the beam at the target

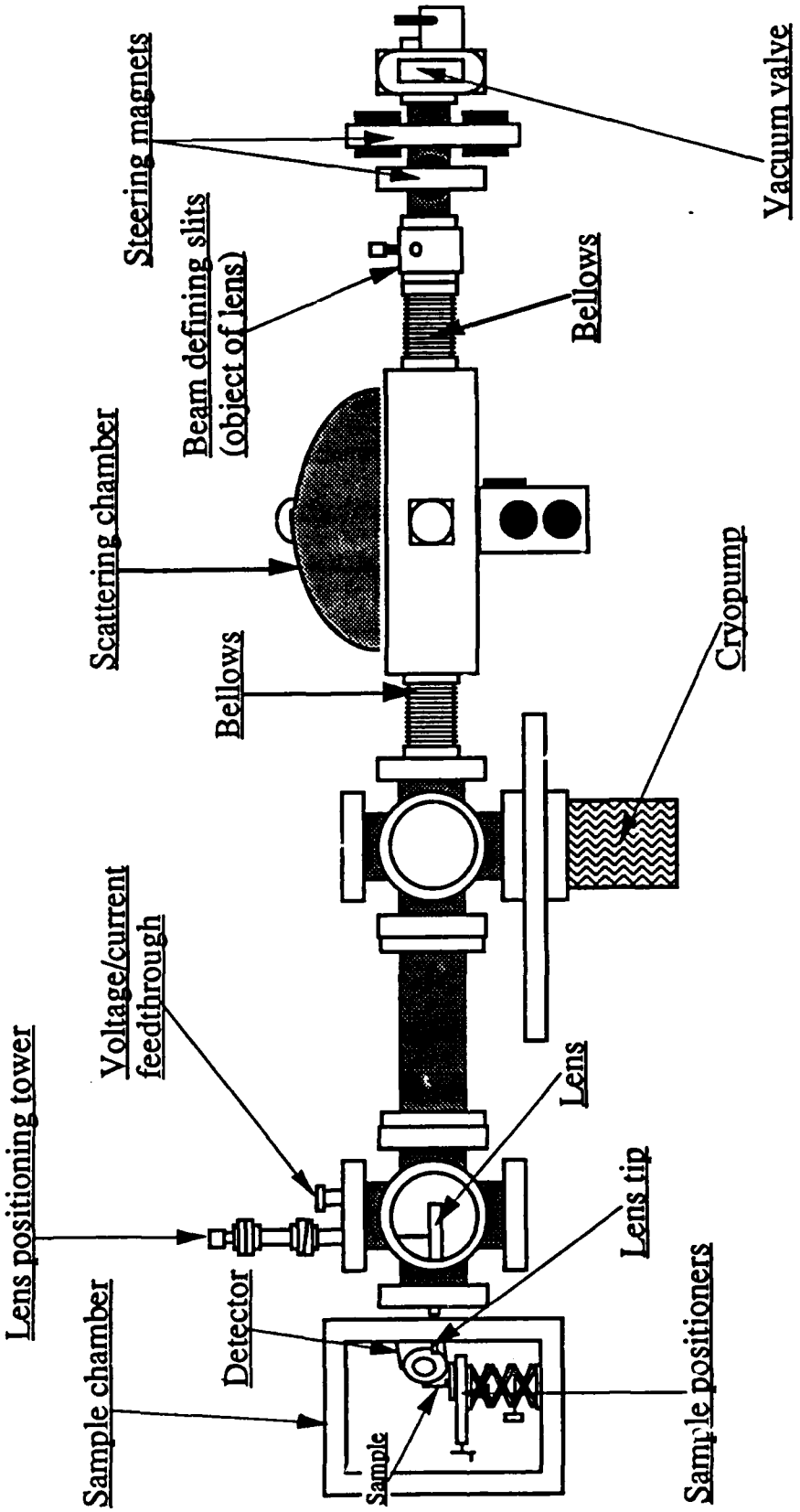

Figure 1: The USNA milliprobe beamline in Michelson C-7. The ion beam from the accelerator enters at the right and is focused onto a target in the sample chamber on the left.

must be known in order to determine the sizes of features in the sample that may be examined accurately. Samples of known concentrations will be analyzed so that the sensitivity of the apparatus may be deduced.

Once the tests have been completed satisfactorily, the equipment is working safely and properly, and the data can be reduced to a conclusive form, efforts can be directed toward the secondary goal of the project, an application of the milliprobe.

2. Design and Construction

2.1 The Electrostatic Quadrupole Triplet Lens

In order for a milliprobe to be effective, the ion beam should be focused to the smallest practical diameter. Doing so allows the milliprobe to select a particular region of the sample and analyze it accurately, as sample features and irregularities can have a width as small as several hundred μm.[11] It also increases the intensity of x-rays in the solid angle viewed by the detector. Unfortunately, unlike a beam of light, a beam of charged particles cannot be focused with a combination of glass lenses. Focusing a particle beam has been accomplished at other accelerator facilities using either magnetic or electric fields. To create this focusing effect for the milliprobe ion beam at USNA, an electric field produced by an electrostatic quadrupole triplet is used.

The electrostatic quadrupole is a set of four parallel metal rods arranged so that their ends form the corners of a square with the beam passing through the middle of the square. This configuration is commonly used, as the circular cross sections of the rods are a good approximation to ideal hyperbolic focusing surfaces.[12] Two of the rods are positively charged and two are negatively charged, with the rods of similar charge placed at the ends of the two diagonals of the square. The lens is enclosed in the beamline vacuum so that the electrodes can be charged to several thousand volts without arcing.

Inside the quadrupole, an electric field is created by the high voltage having equipotential lines that conform to the shape of the poles. A representation of this field along with equipotential lines is given by Figure 2. As stated above, we can approximate this shape, as well as the shape of

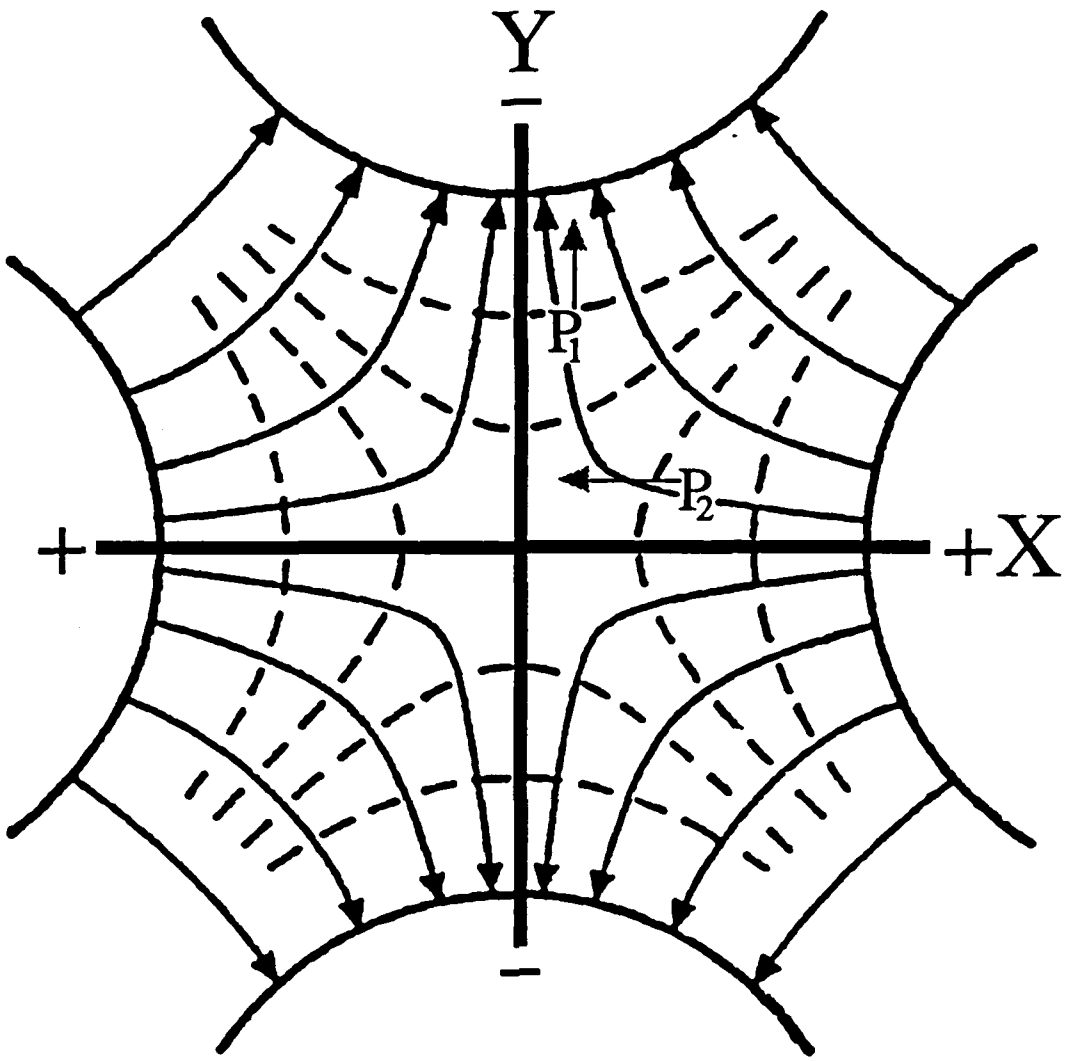

Figure 2: The lines of force and equipotential lines created by the cylindrical electrodes in an electrostatic quadrupole. The particles P_1 and P_2 are positively charged and therefore experience forces in the directions shown. These forces are the basis for the focusing action of the lens.

the lines of force (perpendicular to the equipotential lines), as hyperbolae. If the center of the lens is considered the origin with the x- and y-axes perpendicular to the beam axis, then the equation for the potential at a point inside is that of a hyperbola:

$$V = \frac{1}{2} k (x^2 - y^2) \qquad 2.1.1$$

where k is a constant that depends on the geometry of the lens. The electric field is the negative gradient of the potential, and the components of this field are:

$$E_x = -\frac{\partial V}{\partial x} = -k x \qquad 2.1.2$$

$$E_y = -\frac{\partial V}{\partial y} = k y \qquad 2.1.3$$

Using $\boldsymbol{F = qE = ma}$, the equations for the acceleration in each direction due to this field are:

$$a_x = \frac{d^2x}{dt^2} = \frac{Qk}{m} x \qquad 2.1.4$$

$$a_y = \frac{d^2y}{dt^2} = -\frac{Qk}{m} y \qquad 2.1.5$$

where m is the mass of a charged particle and Q is its charge. Thus, the particles are given components of velocity in the x and y directions in the lens proportional to their distance from the beam axis. These acquired components are what actually "focus" the beam of particles.

Three sets of quadrupoles are typically used to focus the beam in both directions perpendicular to the direction of the beamline. With only one set, focusing in both planes perpendicular to the beamline would not be possible. As shown above, the accelerations corresponding to the two perpendicular axes point in opposite directions with respect to the origin; the result is a "flattening" effect, causing the charged particle beam to

converge in one plane and diverge in the perpendicular plane. The primary disadvantage of a doublet (consisting of two sets of quadrupoles) is that if the system were modeled by a thin optical lens, the position of this lens would be different in the two perpendicular planes, and this difference would vary with the voltage placed on the poles.

A symmetrical triplet is a type of three-element lens with the outer quadrupoles having identical lengths, voltages, and spacings from the inner lens. The converging planes for the outer lenses are opposite the converging plane of the inner lens. This triplet can be modeled as a single thin lens in both perpendicular planes. The position of this lens does not vary with voltage, provided the relative voltage increase is the same for all poles.[13] In order to create electric fields inside the outer elements that are opposite that of the inner element, the inner quadrupole voltages are in a configuration opposite the outer two sets. The inner quadrupole voltages are also higher and the poles are longer in order to compensate and cause the beam demagnification to be the same in both directions.

The USNA milliprobe lens configuration is shown in Figures 3 and 4. Several other laboratories have constructed lenses such as these, and this particular design is a result of considering the advantages and disadvantages of existing lenses. Figure 3 is a side view of the lens illustrating the lengths of the poles and the orientation of the beam. The cross section in Figure 4 shows how the poles are held in their proper positions by specially designed spacers. A similar type of spacer/case design was employed in a quadrupole triplet built by C.P. Swann at the Bartol Research Institute, University of Delaware.[14] The spacers in the USNA lens slide into a stainless steel tube that is the lens case. They are constructed of Macor, a machinable glass, while the spacers in the Bartol lens are made of plastic.

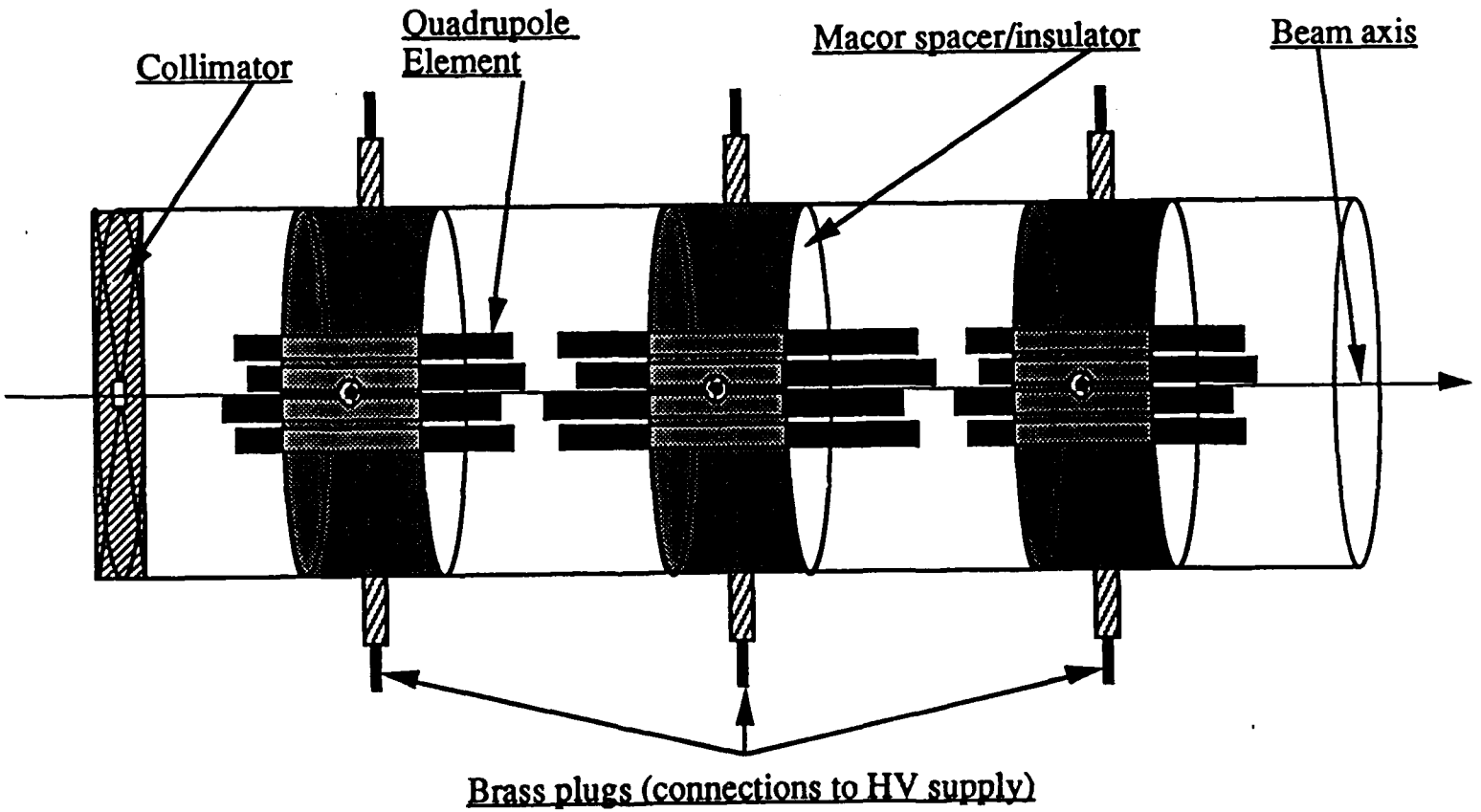

Figure 3: Side view of the USNA electrostatic quadrupole lens. As this is a symmetrical triplet, the outer elements are identical in length, and the inner element is slightly longer. The spacing between the elements is constant.

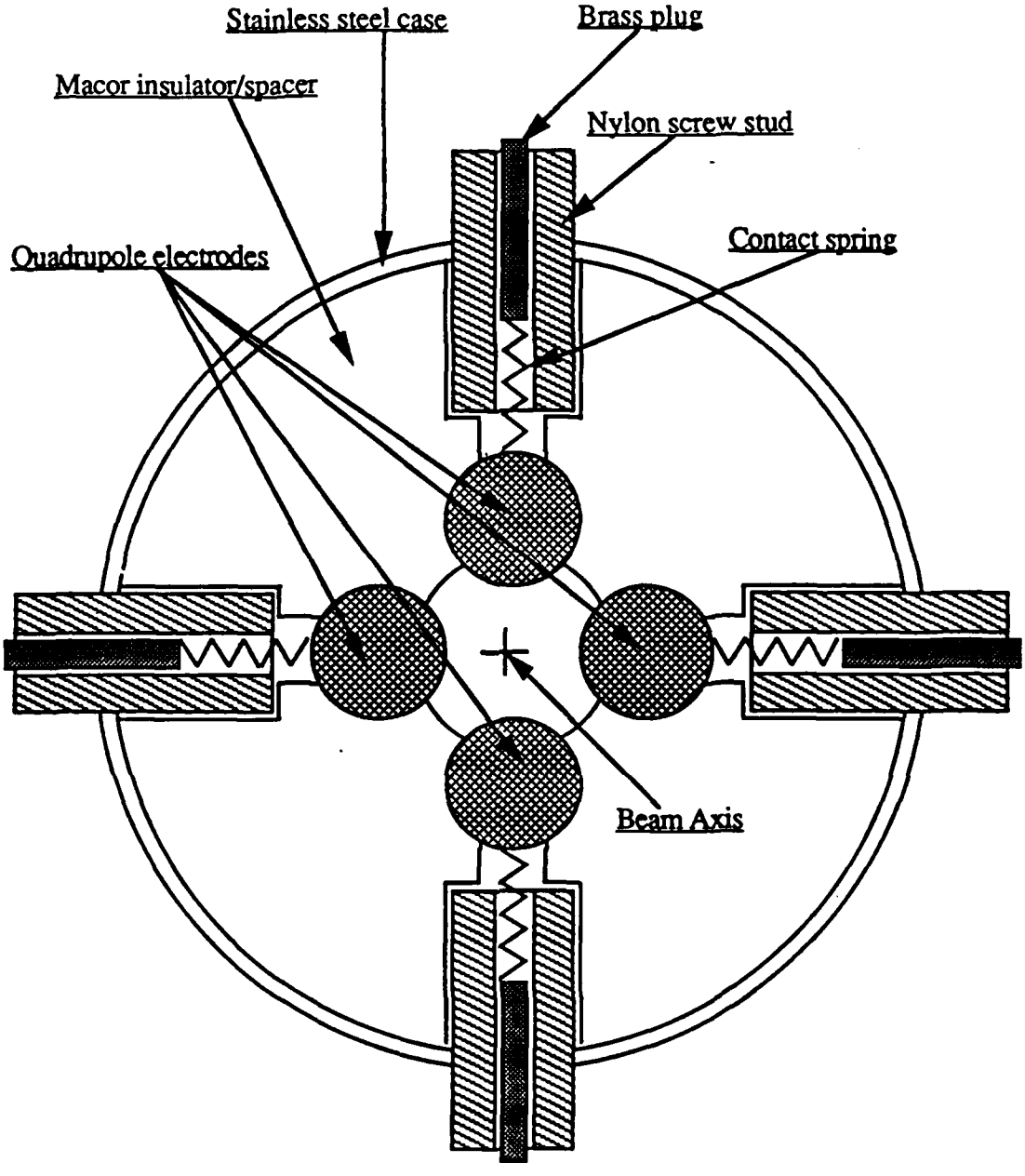

Figure 4: Cross section of a quadrupole element. The voltage is transferred to the quadrupole element through the brass plug/spring connection inside the nylon screw stud.

The Macor insulates the poles from each other and the surrounding case. The spacers are also different from those used in earlier designs, as they have the ratio of the electrode diameter to the bore diameter approximately equal to 1.11. This ratio has been found to most closely approximate the field produced by hyperbolic electrodes and therefore reduce the fringing effects of cylindrical electrodes.[15]

In order to make electrical contact with the poles, watchband springs inserted in hollow screws were used in an electrostatic quadrupole assembly built for Bell Laboratories, Murray Hill, NJ.[16] The Macor spacers in the USNA lens have holes drilled laterally from the outside up to each pole to connect them with the voltage supply. This connection is also made through the use of tiny springs that make contact with the electrode at one end. The difference is that the hollow screws in the USNA lens are made of nylon to insulate the high voltage from the case. Electrical contact is made with a brass rod inserted into one end of the nylon screw that pushes the spring up against the electrodes. Connectors attached to wires that run out of the vacuum chamber are slipped over the rods.

2.2 Lens Positioning System

Due to the nature of the accelerator, it is impossible to predict the exact position of the beam within the beamline. The steering magnets, seen in Figure 1, control the beam and aim it at the lens. If the lens is not correctly aligned along the axis of the beamline, however, it is ineffective, tending to steer the beam as well as focus it. Therefore, it is necessary to be able to accurately orient the lens along the beam from outside of the vacuum chamber.

The lens is supported by a single rod attached to a stainless steel collar that slips around the lens case. There are three separate positioners that control the orientation of this rod inside the vacuum chamber and, subsequently, the orientation of the lens itself. At the top of the "stack" of these devices is a positioner, attached to the other end of the rod, that moves the lens in the vertical direction. This is attached directly to a rotating cuff that permits motion of the lens in the horizontal plane. Below this cuff is the third positioner, which allows a controlled tilt of the entire assembly up to ten degrees in any direction.

2.3 Lens Power Supplies

There are four high voltage power supplies used to apply the necessary high voltages to the lens elements. Two are for the negative and positive poles of the outer elements in the triplet, and two are for the negative and positive poles of the inner element. These power supplies can be remotely programmed by means of a zero-to-minus-five volt signal, and are interlocked with a pressure setpoint on an ionization-type vacuum gauge. The programming voltage is obtained from a voltage controller designed and built as part of this project, especially for the USNA electrostatic quadrupole.

This voltage controller uses two operational amplifiers with potentiometers as the feedback resistors; this is shown by the circuit diagram in Figure 5. The first op amp is in an inverting configuration, and the potentiometer is used to vary the output voltage between zero and minus five volts to control the outer quadrupoles. The second op amp is non-inverting and in this configuration merely amplifies the signal sent to the inner quadrupole. The potentiometer is used to vary this voltage,

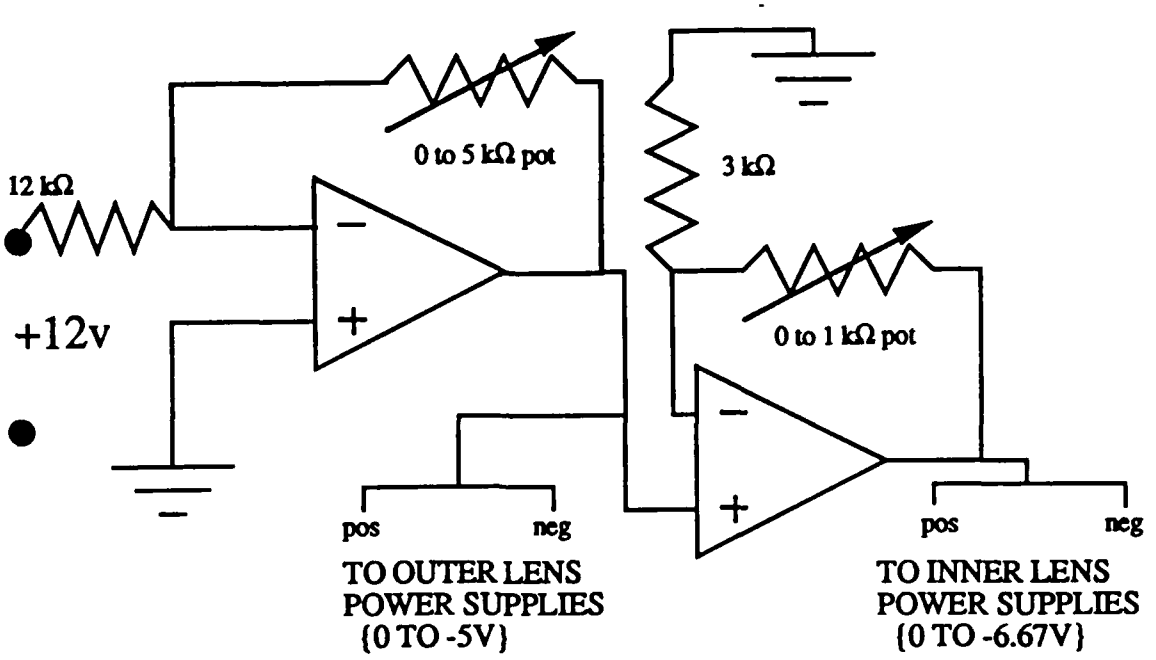

Figure 5: Circuit diagram for the high voltage power supply driver. The 0 to 5 kΩ pot controls the "strength" of the lens, and the 0 to 1 kΩ pot controls the ratio of the inner to outer power supplies.

thereby varying the ratio between the control voltages for the inner and outer quadrupoles. This design is particularly useful for focusing the lens; the first potentiometer adjusts the overall strength of the lens to a value appropriate for the beam energy, and the second adjusts the position of focus for a particular target distance.

2.4 Lens Collimator and Beam Current Monitor

The ultimate goal of the steering magnet/lens positioner combination is a beam that enters the lens on axis. A four-plate collimator mounted on the front of the lens not only keeps the beam from striking the quadrupole elements directly, but also determines where on the lens axis the beam is entering the lens. The plates are arranged to cover four quadrants on the front surface of the lens as illustrated in Figure 6, and each plate is electrically isolated to permit a measurement of the beam current on that quadrant. These currents are then read on the current monitor, another piece of electronic equipment built specifically to be used with the USNA electrostatic lens.

The monitor consists of four sets of two operational amplifiers each, in a combination designed to convert a very small input current into an easily measured voltage. Each of the first of these amplifiers is in a non-inverting configuration modeled after a current monitor built and used at Triangle Universities Nuclear Laboratory. The second amplifier in each set is connected by a switch to a group of three feedback resistors. A single set is illustrated in Figure 7. By simultaneously changing the gain of all four amplifiers, the switch serves as a method to change the sensitivity of the display. Each of the four signals is sent from the amplifier to a corresponding light emitting diode (LED) bar driver, and these drivers

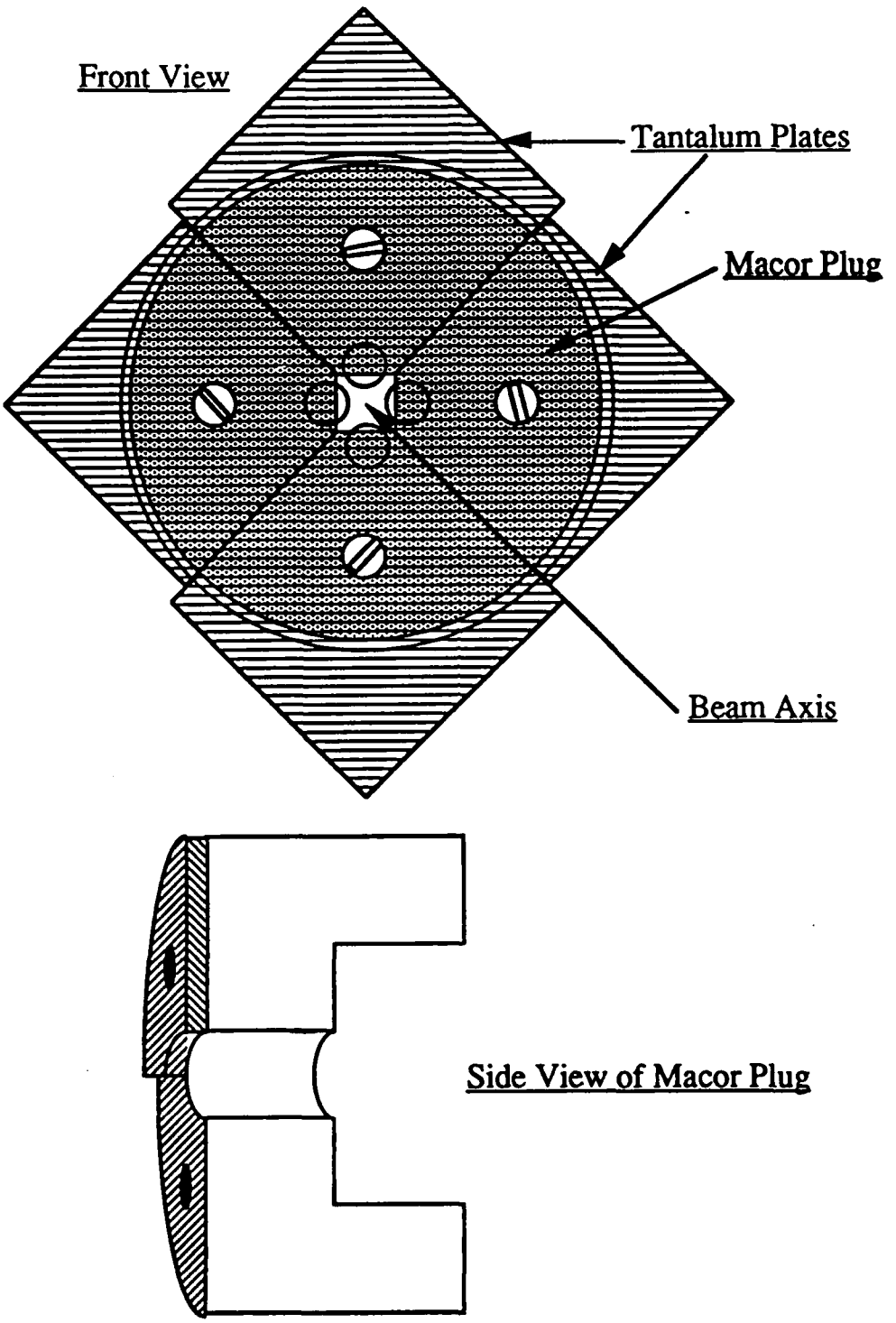

Figure 6: The collimator on the front of the lens is mounted using a macor plug specially designed to electrically isolate the four tantalum plates that recieve the beam current.

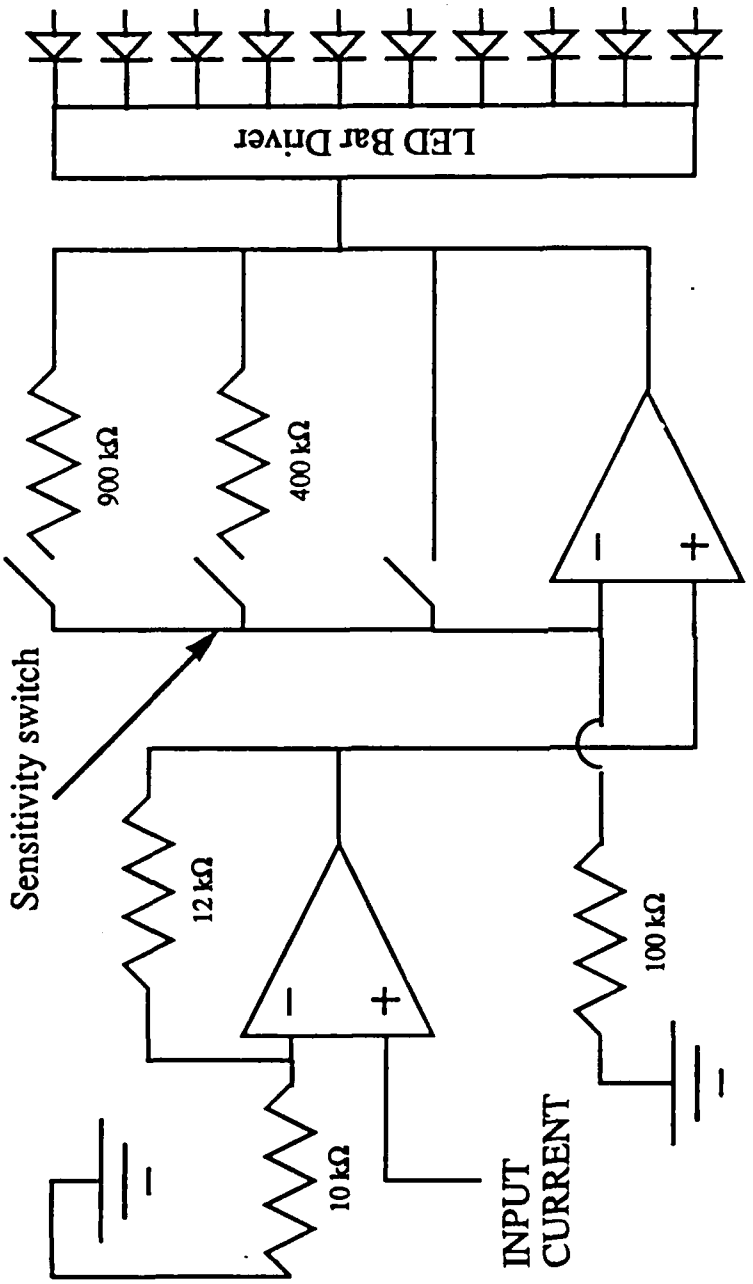

Figure 7: Circuit diagram for the current monitor. Four of these circuits control the 40 LED display on the face of the monitor. By simultaneously changing the gain of all four circuits, a common switch serves to change the sensitivity of the display.

control a display consisting of four bars of ten LEDs each. The LED bars are arranged in a cross-like configuration that represents the arrangement of the four collimator plates as seen by the incoming beam. Thus the LED display produces an accurate and easy to read picture of the current distribution as the beam enters the lens.

2.5 Beam Exit Tip

Once the beam passes through the electric field of the lens, it converges fairly quickly, at a distance of about ten centimeters from the lens exit. Within that distance, it must exit the vacuum of the beamline and strike a target. The compression fitting which holds the exit tip is therefore less than a centimeter away from the lens exit. The exit tip has several additional design constraints. As well as preserving the vacuum in the beamline, the tip should cause minimum attenuation as the beam passes into the atmosphere. Also, any beam particles that strike the tip should not produce high energy x-rays that would interfere with the x-ray spectrum of the target.

The tip, shown in Figure 8, is made from a 0.95 cm outer diameter stainless steel tube with a 0.64 cm inner diameter. Inserted into the steel tube is a 0.64 cm outer diameter carbon rod with an 0.32 cm inner diameter. At the exit end of the tip, the tube surfaces are filed down until they are flush, and a 7.5 μm thick Kapton foil is attached to this surface with vacuum epoxy. Because carbon has a very low atomic number, any x-rays produced by beam collisions with the interior of the beam tip will be at a low enough energy so as not to interfere with the spectrum of the target. The thin Kapton foil is also composed of light elements (H, C, N, and O) to reduce high energy x-ray production. It is strong enough to hold

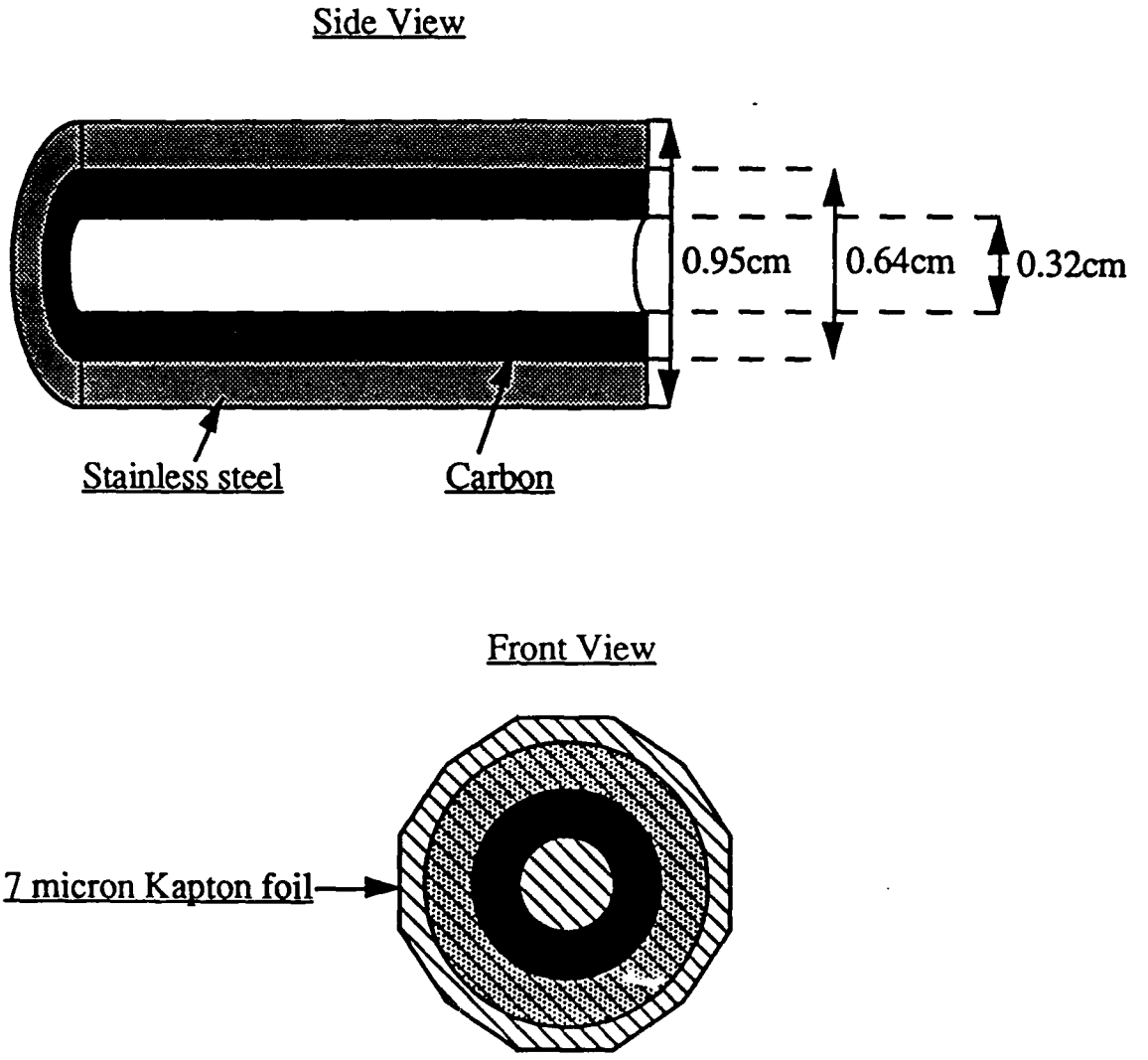

Figure 8: The tip through which the beam exits is constructed from a 0.95cm diameter steel tube with a 0.64cm diameter carbon rod inserted inside it to prevent high energy x-rays produced from the beam colliding with the steel. The Kapton foil covering the end is strong enough to hold the vacuum of the beamline while still permitting protons to escape.

up under the beam current and the pressure differential between the vacuum of the beamline and the atmosphere.[17]

2.6 Sample Enclosure

A structure to enclose the space in which the beam exits the vacuum, strikes the sample, and is detected, is needed for several reasons. First, to prevent human contact with the external beam, the hinged panels on the enclosure are interlocked with a valve in the beamline. Second, the chamber can be filled with helium gas. Helium does not attenuate the beam and subsequent x-rays produced in the sample as much as air does, and immersing the sample in helium gas increases the sensitivity of the technique. Finally, the chamber is an extension of the framework supporting the beamline, and its bottom panel serves as a convenient location to mount the device on which the sample is positioned.

This device consists of a lab jack fastened to the bottom of the chamber that is used to raise and lower the sample. Mounted on top of the stand is a lateral positioner to move the beam horizontally across the target. The sample is mounted with its surface perpendicular to the beam axis and at a 45° angle with respect to the vertical. A more compact x-y positioner built for smaller increments of motion may be added if the need for scanning exact portions of the sample arises.

In order to minimize the distance that the beam and the x-rays travel through the air, the detector is supported at the roof of the sample enclosure causing it to point directly down at the sample. Mounting the detector horizontally behind the enclosure proves to be inadequate as the axis of the detector does not intersect the point at which the beam strikes the sample. If the detector is slightly repositioned to correct this geometry,

both the ions and the x-rays are greatly attenuated by the increased path length in air. The angle between detector and beam axis is therefore 90°, hence the 45° angle of the sample mount. The sample mount can then be placed very close to the exit foil (approximately 0.5 cm). Slipped around the end of the detector is a lightweight plastic sleeve. This serves as a hood into which the helium is introduced, rising and displacing the air. The sample is raised up into the hood to position it in front of the beam tip, resulting in a detector to sample distance of approximately 1 cm and a relatively large detector solid angle.

3. Testing and Calibration

3.1 Aligning the Beam

If the ion beam optical elements such as apertures and the lens are to perform their desired functions, the beamline must be aligned parallel to the beam along its entire length from the accelerator to the sample chamber. Because the beam is invisible to the naked eye, it is very difficult to determine its precise position in the beamline. If the beam is not centered in the pipe, it will not be properly controlled by the beam optics, and it may even strike the beampipe at some point before the lens, depositing all of its energy onto the pipe.

One method of locating the position of the beam is to insert quartz disks into the beamline; quartz produces a blue fluorescence when struck by the beam. That part of the beamline from the analyzing magnet to the scattering chamber was aligned by disconnecting the bellows and insulator and capping the beamline off with a special flange containing such a quartz disk. The beamline supports were then adjusted until the blue spot was centered on the quartz.

Included in that portion of the beamline were the collimator and the steering magnets. Once the supports were adjusted, the collimator slits were closed down to form an aperture one millimeter on a side, creating an object in the beam for the lens. The steering magnets were adjusted until a minimum beam current was striking both the horizontal and vertical slits. This alignment ensured that the maximum amount of beam current passed through the aperture and was focused by the lens.

In order to align the remaining portions, the beamline was reassembled. A quartz disk was placed on one of the rotating arms in the

scattering chamber, and another was mounted on a mechanical feed-through in the cross above the cryopump. In order to view these, the opaque metal dome on the scattering chamber was replaced by a thick transparent plexiglass disk, and a plexiglass window took the place of one of the panels on the cryopump cross. The beamline support frame was gently "nudged" until the beam spot appeared centered horizontally on the quartz disks. The chamber and beamline supports were then adjusted to center the beam horizontally.

One final tool for beam alignment was the current monitor connected to the lens collimator. Initially, the lens was optically aligned with the beamline by focusing a telescope through the transparent Kapton foil onto a set of crosshairs. These crosshairs were placed over the beamline entrance to the scattering chamber. Once the quartz disks were removed from the path of the beam, the cross-shaped LED display on the current monitor indicated the position of the beam at the lens. The lens chamber supports were subsequently adjusted to bring the entire beamline, from object collimator to exit tip, into alignment.

3.2 External Beam Focus and Measurement

To ensure that the alignment was complete, a zinc sulfide screen was placed on the sample mount and positioned directly in front of the exit tip. Zinc sulfide fluoresces when it is struck by the beam, indicating the size and shape of the beam at that point in the air. At first the spot seemed faint and eclipsed; this was remedied by adjustments to the lens positioners and steering magnet currents. After several iterations of these adjustments, a rectangular image similar in shape to the opening of the lens collimator appeared on the screen.

An initial focusing of the beam with the electrostatic quadrupole lens was performed using the screen. Both the strength and ratio controls were slowly increased until the beam spot appeared to reach a maximum density. It is important to note that during this procedure, the screen was approximately one centimeter from the exit foil. At distances much greater than 1.5 centimeters from the foil, a strong focus on the screen did not appear to be obtainable, probably due to the attenuation of the beam in the air. The strength and ratio dials read 1.65 and 5.00 respectively for this initial focus. These readings correspond to 825 volts on the outer elements and 1015 volts on the inner element.

The technique used for measuring the width of the external beam consisted of stepping a 36 gauge copper wire through the beam at precisely measured intervals on the order of 100 μm. This type of measurement has been employed before to determine the width of much smaller diameter external beams.[18] The copper x-rays were counted for each wire position with the MCA. In order to normalize each counting run to the same number of protons entering the lens, a thin carbon film was inserted into the beamline in the scattering chamber. There, a certain percentage of the protons were scattered by the ^{12}C nuclei, detected, and counted. The counter/timer was set for 5000 counts, at which point it would send a signal to the multi-channel analyzer (described in section 4.2) that would shut out the signal from the x-ray detector.

A run was made with the lens turned off, and another was made with the lens voltages set at the optimum values for focusing the beam. The results of both runs are shown in Figure 9, to illustrate the effect on the beam profile. The most striking difference between the two profiles is the number of counts at beam center (35000 as compared to 95000) which

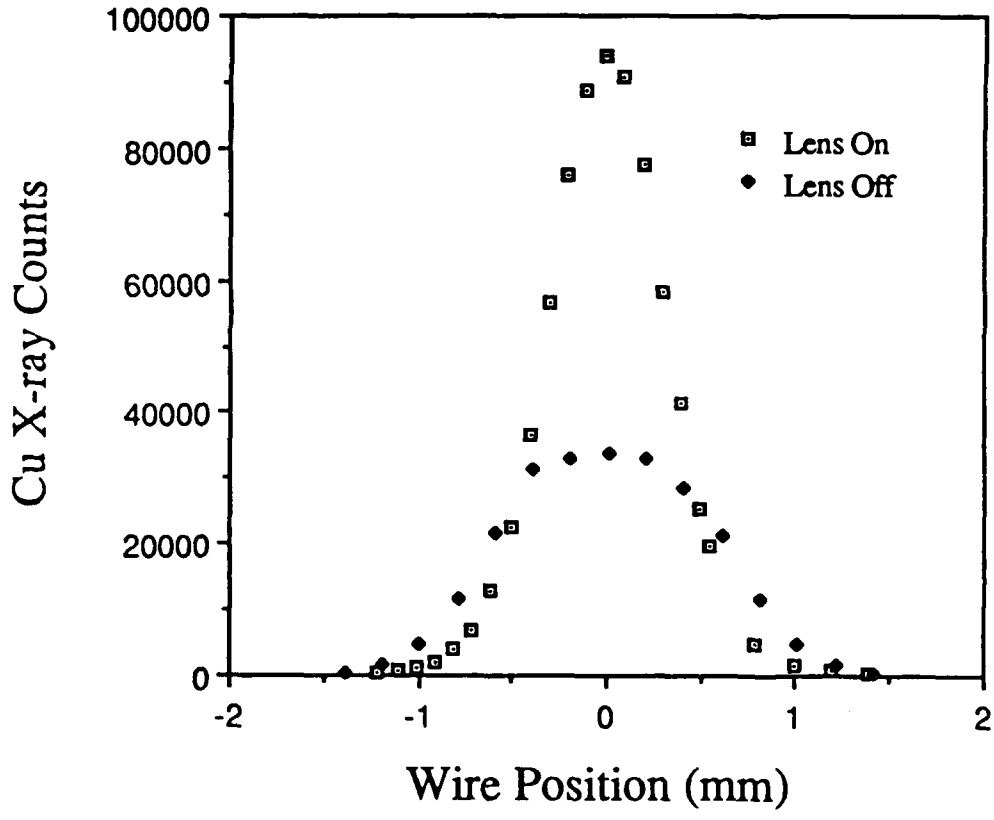

Figure 9: This graph was produced by stepping a copper wire through the beam at precise intervals of 100μm. The two peaks demonstrate the effect of the lens on the external portion of the beam.

depends directly on the intensity of the beam on the wire. The full width at half maximum (FWHM) of the peaks corresponds to the diameter of the beam spots at the wire. On a relative scale, the FWHM of the "Lens On" peak was less than 50% of the "Lens Off" peak. The measurements therefore demonstrate that the lens reduced the size of the beam spot while increasing its intensity in the area of the sample illuminated by the beam.

4. PIXE Analysis

4.1 Theory

The PIXE technique involves the interactions of energetic beam protons with the atoms of a target sample. As a simplified model, a target atom can be described as a tiny point-like nucleus surrounded by electrons orbiting the nucleus at different levels. These levels represent the different energy states of the atomic electrons. Because these electrons are bound to the atoms by energies on the order of ten electron volts, a two-MeV proton is easily able to knock the electron out of its orbit and away from the atom, as shown in Figure 10. This creates a vacancy in the electron orbits surrounding the atom, and the other electrons "cascade" downward in their energy levels to fill in this vacancy. As a result, the excited atoms release energy in the form of an x-ray photon.

Atoms of the different elements have different nuclear charge and numbers of electrons and therefore unique arrangements of the orbiting electron energy levels. For example, when an electron in an iron atom makes a transition from level A to level B, it produces an x-ray of a wavelength different from that of an aluminum electron making transitions between the same levels. These x-rays are then absorbed by the x-ray detector through a variety of processes depositing charges within the detector. These charges produce signal pulses that are counted and displayed on the multi-channel analyzer (MCA).

4.2 The Multi-Channel Analyzer

The specific type of MCA used for this project is a personal computer application produced by The Nucleus, Inc. It consists of a circuit

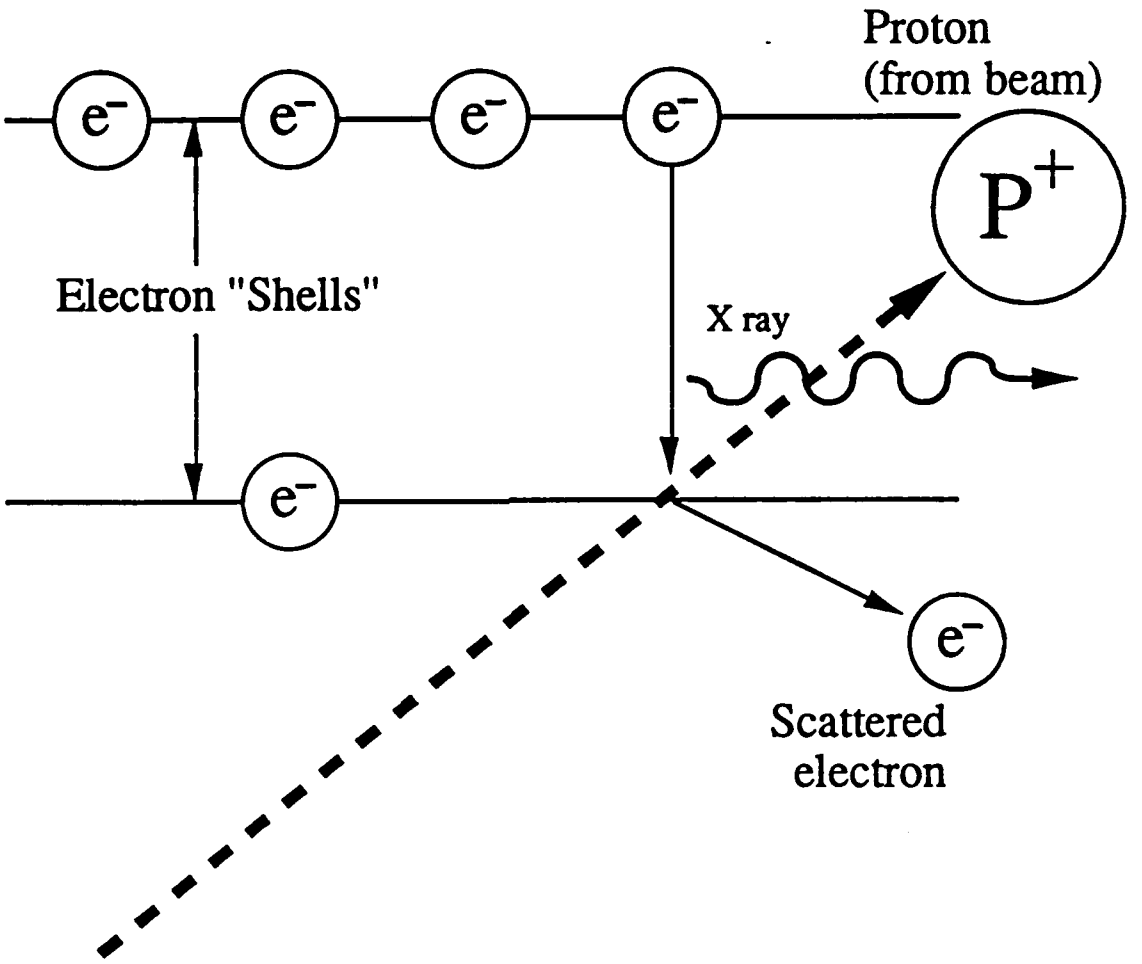

Figure 10: The PIXE mechanism - an incident proton knocks an electron out of its shell causing electrons in the higher orbital to fill in the gap. In order to transit to this lower energy level, the electron must give up energy in the form of an x-ray.

card and some accompanying software that are installed in a Zenith 248 microcomputer. When the detector is connected and active, a graph with the energy of the pulse as its x-axis and the number of pulses or counts as its y-axis is displayed on the monitor (see Figure 11). The result is a spectrum that contains peaks at the energies, or channels, of the detected x-rays. The width of a peak corresponds to the detector resolution; the detector is not able to match every identical x-ray with exactly the same size pulse and spreads the peak corresponding to the particular x-ray across several channels.

4.3 Data Reduction Software

Knowing the energies of the characteristic x-rays corresponding to each atom, it is possible to ascertain the elements present in that portion of the sample being struck by the beam. The MCA is able to highlight the K, L, and M x-ray energies for a specified element on the spectrum display. Unfortunately, the MCA is only a tool for counting the pulses produced by the x-rays and keeping track of their energies. This display is inadequate for the purposes of determining sample concentrations, since the relative heights of the peaks are affected by factors such as background, attenuation, and fluorescence yield that depend on the energy of the x-ray but are not dealt with by the MCA software. The MCA also does not account for peaks that are the result of two or more elements with overlapping x-ray energies.

The data set is therefore converted[19] and sent to a computer program to be analyzed for elemental concentrations. The program adopted for the milliprobe is known as PIXAN PC[20], developed by the Australian Atomic Energy Commission. This computer program is designed to

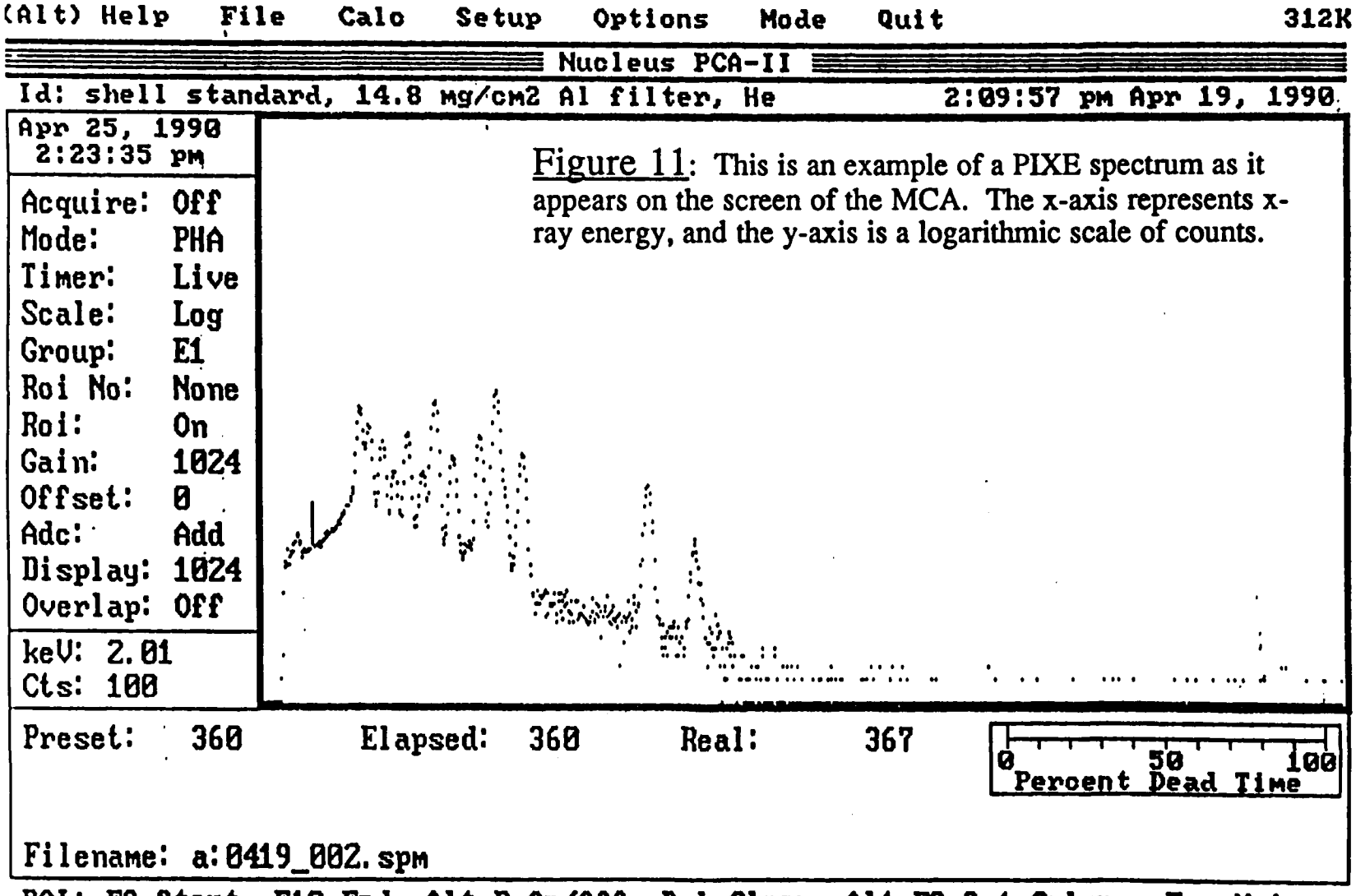

Figure 11: This is an example of a PIXE spectrum as it appears on the screen of the MCA. The x-axis represents x-ray energy, and the y-axis is a logarithmic scale of counts.

mathematically fit several types of functions to the experimentally measured x-ray spectrum in order to separate the data into peaks resulting from each individual element.

The first function is a polynomial that is meant to describe the background radiation and separate it from the x-ray peaks. The individual peaks are then fitted with gaussian functions having centroids located at the energies of the x-rays that are produced by the corresponding element. Information concerning the order of the background polynomial is given as input to the program. In addition, the program can be told to compensate for attenuation due to a filter between the sample and detector. This is an important function, since thin filters of light materials such as beryllium and aluminum are often necessary to attenuate the relatively intense light element x-rays so that those from the heavier elements can be seen.

5. Testing and Preliminary Analysis

5.1 Preparation of an Oyster Shell Standard

An effective way to evaluate the sensitivity of any elemental analysis technique is the use of a standard sample of known concentration. In anticipation of the USNA milliprobe's eventual study of oyster shells, an "oyster shell standard" was created in accordance with a chemical recipe for the composition of a typical oyster shell.[21] The recipe and the resulting concentrations by number of the heavier elements are listed in Table 5.1. The required chemicals were measured and ground together with a mortar and pestle. A small amount of this mixture was then further blended using a "wiggle bug", a small cylinder in which the chemicals are mixed by a ball bearing to produce a homogeneous sample. The resulting mixture was placed in a hydraulic press and made into a small pellet that could be easily positioned in front of the external beam.

5.2 Analysis of Standard and Shell

Before any spectra were taken of the standard, the beam was once again focused on the zinc sulfide screen. The first spectrum of the standard, shown in Figure 12, demonstrates the need for a filter between the sample and the detector. Because an enormous number of low energy x-rays bombards the detector during each fraction of a second, a pair of photons is sometimes counted simultaneously and their energies are added together to form a "sum peak". This peak is most prominent around 7 keV, about twice the energy of a calcium Kα x-ray.

The filter chosen to correct this problem was a 14.8 mg/cm^2 aluminum foil. Aluminum has a K absorption edge at 1.559 keV; this is a

Table 5.1: Recipe for the Shell Standard

$CaCO_3$	20.0g
S_8	0.4g
TiO_2	0.5g
CrO_3	0.3g
Fe_2O_3	0.2g
$CuCl_2$	0.4g
$ZnCl_2$	0.4g
$SrCl_2$	0.4g

Resulting Number Concentrations of the Heavier Elements

Ca	17.75%
Fe	0.22%
Cu	0.21%
Zn	0.26%
Sr	0.13%

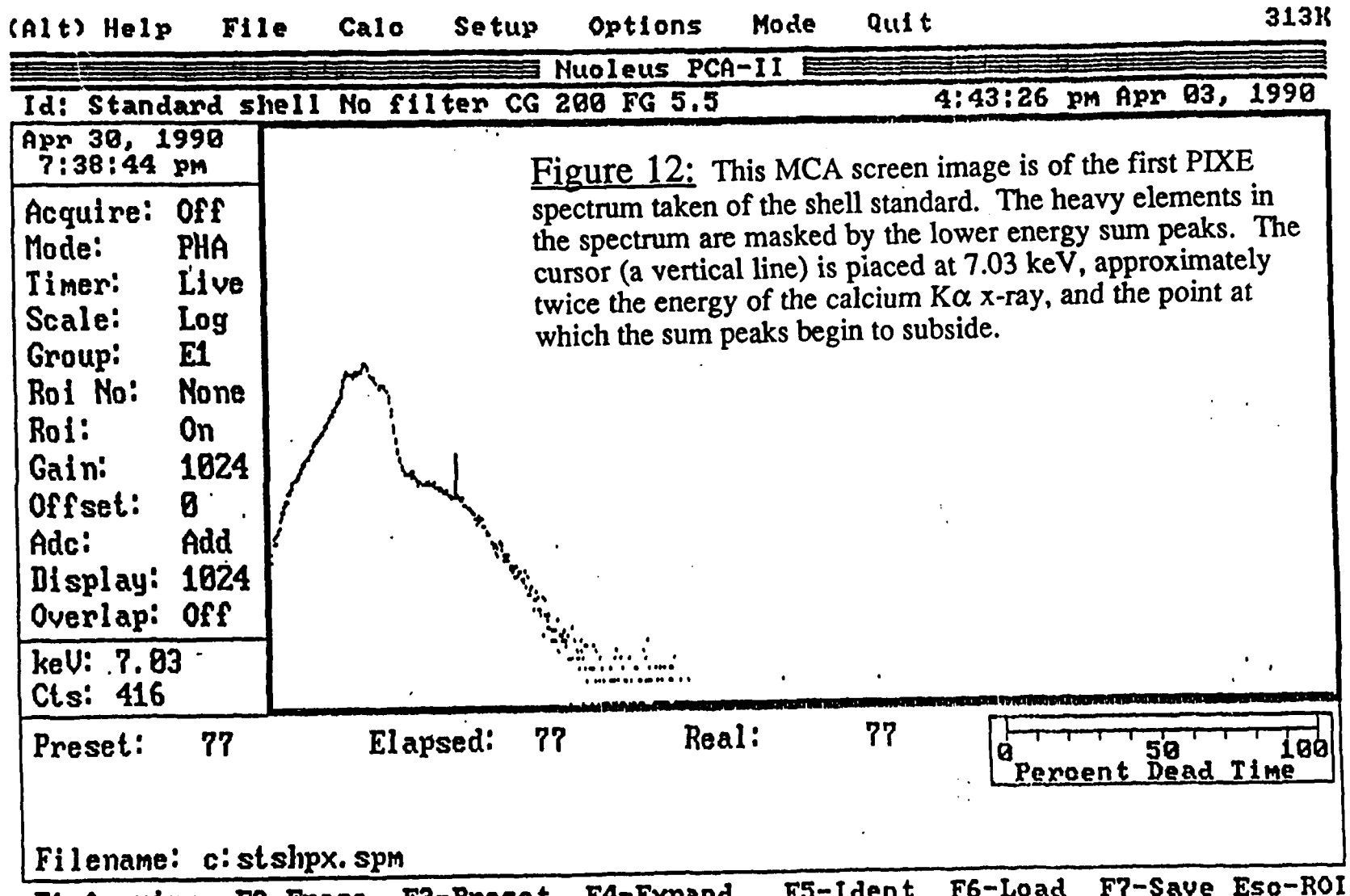

Figure 12: This MCA screen image is of the first PIXE spectrum taken of the shell standard. The heavy elements in the spectrum are masked by the lower energy sum peaks. The cursor (a vertical line) is placed at 7.03 keV, approximately twice the energy of the calcium Kα x-ray, and the point at which the sum peaks begin to subside.

peak in the attenuation coefficient curve that causes the aluminum atom to strongly absorb x-rays immediately above 1.559 keV. This energy is low enough to strongly filter out the abundance of x-rays from the lighter elements, and thin uniform foils are readily available. The spectrum that resulted from the addition of this filter is the example MCA screen illustrated in Figure 11. Using the same filter, the sample was replaced by a real oyster shell and two spectra were taken at different locations on the shell. This data set was saved to disk and converted to a PIXAN PC input file.

The PIXAN PC program first required information about the detector resolution and energy calibration. These were obtained from a spectrum taken of ^{57}Co deposited on a palladium foil, a source that emits photons at 6.400, 7.059, 14.412, 21.123, and 23.859 keV. The other inputs required by PIXAN PC dealt with an estimate of the expected composition of the sample. A list of the major elements in the sample along with their approximate relative concentrations by weight was used to correct for self absorption. This is the absorption of x-rays, created within the sample, by atoms of the sample itself. Finally, a "shopping list" of elements that were reasonably believed to be in the sample was given to save time during the run. The program will not try to fit any elements that are not included in this list.

Three initial runs were made; one for the shell standard and one at two different locations on an actual shell. The results of the shell standard run are plotted in Figure 13, and the actual shell for the first position in Figure 14. In both of these plots, the data spectrum is represented by a solid line, the peak fit by a dashed line, and the background fit by a dotted line. In addition to these plots, an output file was created that included the

input data, the peak areas of the fit for each element, the value of χ^2 (a goodness of fit parameter) for each element, and the minimum detection limits for each element fit. At first, the same shopping list of elements used in the shell standard was given to the actual shell runs, and the program failed to find any titanium or chromium as were present in the standard. There was, however, an obvious peak at a slightly lower energy than iron that the code was clearly not trying to fit. When manganese was added to the shopping list, the spectra were re-fit with considerably better results.

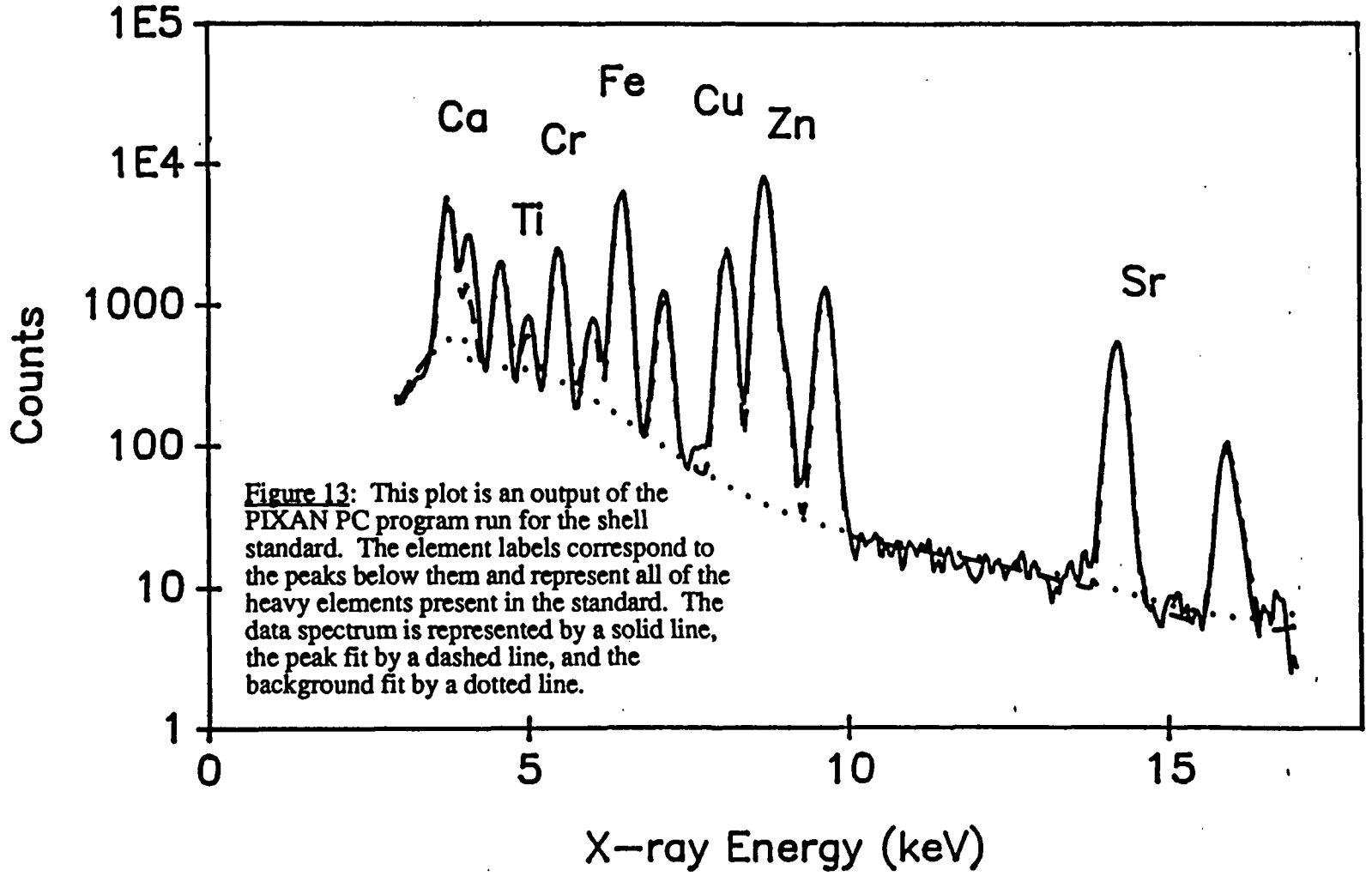

Figure 13: This plot is an output of the PIXAN PC program run for the shell standard. The element labels correspond to the peaks below them and represent all of the heavy elements present in the standard. The data spectrum is represented by a solid line, the peak fit by a dashed line, and the background fit by a dotted line.

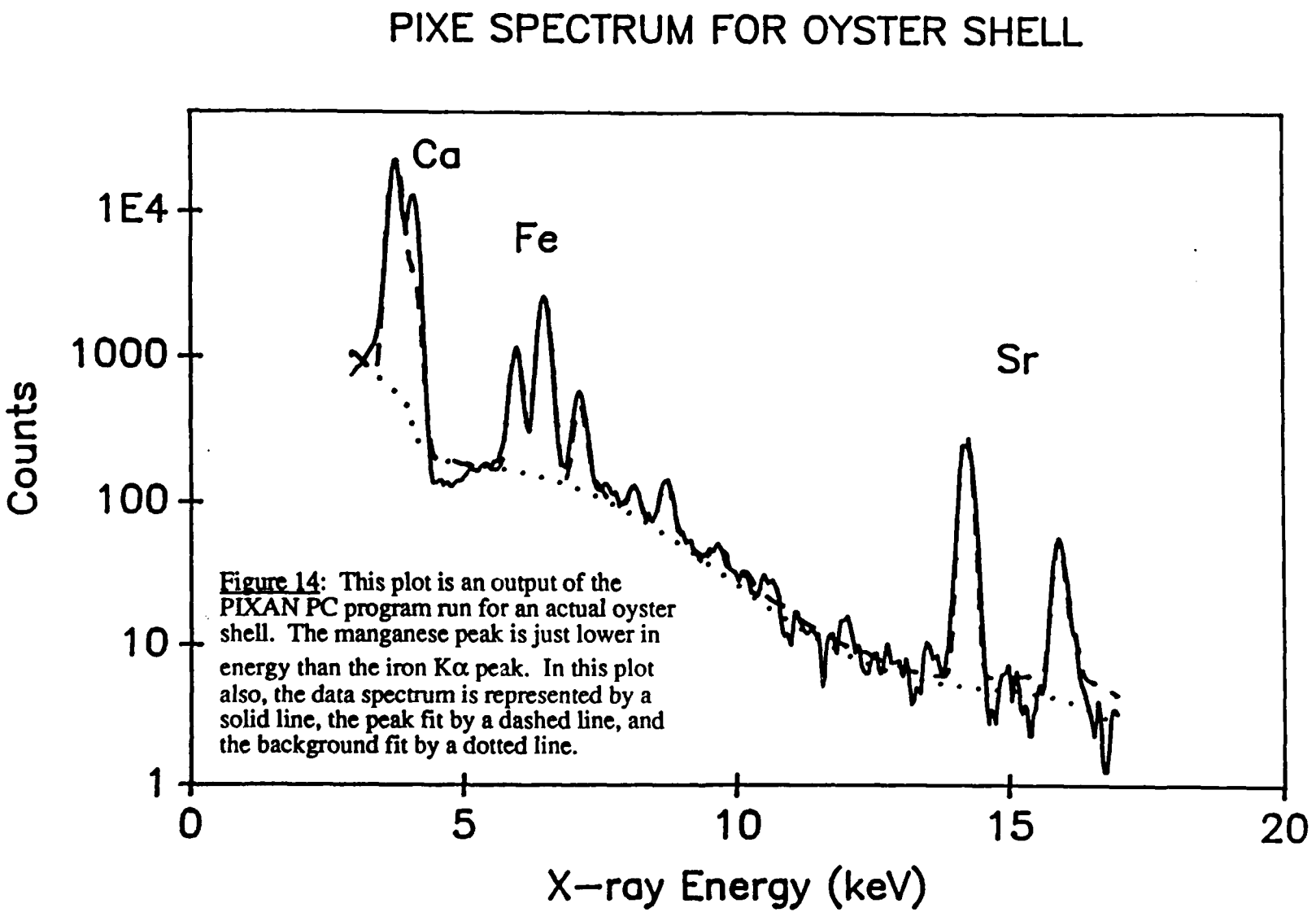

Figure 14: This plot is an output of the PIXAN PC program run for an actual oyster shell. The manganese peak is just lower in energy than the iron Kα peak. In this plot also, the data spectrum is represented by a solid line, the peak fit by a dashed line, and the background fit by a dotted line.

6. Conclusion

6.1 Results and Implications

There are in fact two parts to the PIXAN PC software. The peak fitting routine described and applied above is known as BATTY, while a more sophisticated composition analysis program known as THICK has yet to be employed. THICK is designed to take the peak areas produced by BATTY and calculate actual concentrations for each element fit.[22] For the preliminary analysis, however, approximations can be made to the actual concentrations in the shells for those elements that were also present in the standard sample.

A peak area that has been calculated by the BATTY program for an element i is a function of several variables:

$$A_i = \phi \times C_i \times \sigma_i \times \alpha_i \times \varepsilon_i \qquad 6.1.1$$

where A_i is the BATTY peak area for element i, ϕ is the number of protons incident on the sample, C_i is the concentration of element i in the area of the sample illuminated by the beam, σ_i is the probability that element i will emit x-rays, α_i is the attenuation of x-rays from element i in the sample itself and in the medium between the sample and detector, and ε_i is the detector efficiency for these x-rays. The equation can be rewritten:

$$\frac{A_i}{\phi C_i} = \sigma_i \times \alpha_i \times \varepsilon_i \qquad 6.1.2$$

Making several assumptions, the right-hand side of the equation has the same value for both the standard and the sample. The concentrations of the major constituents of both the standard and the shell (primarily calcium, carbon and oxygen) were taken to be approximately equal in order to neglect any difference in self absorption and x-ray yield probability

between the two samples. The very good assumption that there were no changes in detection geometry was also made in order to rule out any differences in external attenuation and in detector efficiency. Accepting the conditions above, the peak areas, numbers of incident protons, and concentrations can be equated as follows:

$$\left(\frac{A_i}{\phi C_i}\right)_{standard} = \left(\frac{A_i}{\phi C_i}\right)_{sample} \qquad 6.1.3$$

To allow for the fact that different samples may have been exposed to different numbers of incident protons, it is common to normalize the concentrations of the various elements to the concentration of a single element in the standard and sample. Since Ca is the major constituent of the standard as well as the shell samples, a special case of equation 6.1.3 is:

$$\left(\frac{A_{Ca}}{\phi C_{Ca}}\right)_{standard} = \left(\frac{A_{Ca}}{\phi C_{Ca}}\right)_{sample} \qquad 6.1.4$$

where $\phi_{standard}$ and ϕ_{sample} are identical to those in equation 6.1.3. Equations 6.1.3 and 6.1.4 can now be divided to eliminate both $\phi_{standard}$ and ϕ_{sample}. The result can be rearranged to give the relative concentration of element i to that of Ca in the sample in terms of the same ratio in the standard and the ratio of two relative peak areas:

$$\left(\frac{C_i}{C_{Ca}}\right)_{sample} = \left(\frac{C_i}{C_{Ca}}\right)_{standard} \times \frac{(A_i/A_{Ca})_{sample}}{(A_i/A_{Ca})_{standard}} \qquad 6.1.5$$

Table 6.1 shows the resulting normalized concentrations for the shell in two positions.

This preliminary analysis shows that, relative to calcium, there was slightly more iron, copper, and zinc, but slightly less strontium, in the second portion analyzed than there was in the first. With a technique such as this, a series of shells containing the elements above could be analyzed

Elt	Standard C_i	Standard C_i/C_{Ca}	Standard A_i	Shell p-1 A_i	Shell p- 2 A_i	Shell p-1 C_i/C_{Ca}	Shell p-2 C_i/C_{Ca}
Ca	2.00E-01	1.00E+00	28379	43905	159387	1.00E+00	1.00E+00
Fe	2.53E-03	1.27E-02	37031	3468	15884	6.05E-02	7.64E-02
Cu	2.36E-03	1.18E-02	14598	57	310	2.52E-03	3.78E-03
Zn	2.91E-03	1.46E-02	50820	114	596	1.45E-03	2.09E-03
Sr	1.48E-03	7.40E-03	3807	673	1829	1.14E-01	8.55E-02

Table 6.1: Preliminary PIXE compositional analysis of two portions of an oyster shell. The three columns under the heading Standard refer to the atom concentration C_i (in moles), the ratio to Ca concentration, and the area A_i under the characteristic x-ray peak for each of the indicated elements present in the "shell standard".

and conclusions drawn as to trends or correlations among these elements. With the employment of a more powerful method such as THICK, however, the data gained by the milliprobe will lend to extremely extensive and accurate results.

6.2 Goals Accomplished

As this Trident Project was for the most part a design project, emphasis was placed on combining the desired requirements for the USNA milliprobe with the knowledge of existing ion beam milliprobes. With this in mind, previous designs were studied for beam focusing lenses, lens positioners, and methods to extract an external beam. Original designs were implemented, however, for the electronic systems - the lens power supply controller and the lens entrance current monitor, as well as the sample chamber and its interlocks. The painstaking process of aligning each of the components of the milliprobe beam line could also be classified under the heading of construction.

The milliprobe was tested in several ways. The focus of the external beam was first visually examined on the zinc sulfide screen and then measured quantitatively with a copper wire. The shell standard was created and the first PIXE spectra were examined on the MCA for the presence of the known ingredients. These spectra, along with some spectra taken of actual shells, were processed by the PIXAN PC program. The results of the shell standard peak fit were used to make some preliminary determinations of the actual shell concentrations.

6.3 Continuing Use of the Milliprobe

The secondary goal of the project was to apply the milliprobe to a problem that required data analysis. In order to arrive at any comprehensive conclusions from such an application, this analysis will entail the utilization of the THICK program. Once THICK is able to efficiently convert the peak areas to concentrations, the milliprobe will be ready for a wide variety of applications. During the course of this project, several proposals were made that were highly feasible for the present configuration of the USNA milliprobe.

The first, as previously indicated, is the analysis of a series of oyster shells. The Maryland Historical Trust has in their possession a collection of oyster shells to which they have assigned dates through archaeological processes. The primary component of the oyster shell is calcium carbonate, which is involved in a variety of chemical reactions. These reactions with the elements in the shell's environment take place as the oyster transports the surrounding water through its valves[22] An elemental analysis of the dated shell will therefore reveal information about the elements in the water during the lifetime of the oyster. A large, cataloged series of analyses such as the USNA milliprobe is able to perform would create a comprehensive database of soil concentrations in the region containing the shells.

Another application includes the analysis of marble samples for the National Gallery of Art in Washington, D.C. An elemental analysis of a marble sculpture may reveal important information concerning the origin of the marble, and this information may be used to link sculptures of unknown origin to their artists. This type of rapid, non-destructive analysis is well suited for the USNA milliprobe. In addition, the primary

component of marble is calcium, so the detector filter could be reused for these spectra.

Accordingly, another Trident Scholar Project has already been created to apply the milliprobe to these and other such analyses. A micro-VAX minicomputer has been procured for the 1990-1991 academic year to increase the data reduction ability and therefore the output of the technique. The versatility of the instrument will allow various research groups with interests in elemental analysis, both at USNA and elsewhere, to obtain the desired results without lengthy preparation.

REFERENCES

[1]K. Maeda et al., "Diagnosis of River Pollution by PIXE," Nuclear Instruments and Methods in Physics Research B22 (1987): 456.

[2]Cahill, T.A., "Proton Microprobes and Particle Induced X-ray Analytical Systems," Ann. Rev. Nucl. Part. Sci. 30 (1980): 211

[3]Cahill, 212.

[4]G. Amsel et al., "MeV Ion Beam Techniques: An Outline," Nuclear Instruments and Methods in Physics Research B14 (1986): 30.

[5]J.W. McMillan, "Nuclear Microprobe Applications in Materials Science," Nuclear Instruments and Methods in Physics Research B30 (1988): 474.

[6]H. Blank and K. Traxel, "Proton Induced X-Ray Emission in Micro-Regions Applied in Mineralogy," Scanning Electron Microscopy III (1984): 1089.

[7]Maeda, 456.

[8]B.H. Kuslo and R.N. Schwab, "Historical Analysis by PIXE," Nuclear Instruments and Methods in Physics Research B22 (1987): 401.

[9]Amsel, 32.

[10]Evan T. Williams, "PIXE Analysis with External Beams: Systems and Applications," Nuclear Instruments and Methods in Physics Research B3 (1984): 211-212.

[11]S.H. Sie and C.G. Ryan, "An Electrostatic 'Russian' Quadrupole Lens," Nuclear Instruments and Methods in Physics Research B15 (1986): 664.

[12]M. Loren Bullock, "Electrostatic Strong Focusing Lens," American Journal of Physics 23 (1955): 264.

[13]E. Regenstreif, "Focusing with Quadrupoles, Doublets, and Triplets," Focusing of Charged Particles, Albert Septier, ed. (New York: Academic Press, 1967) 389.

[14]S.J. Flemming, and C.P. Swann, "The Bartol PIXE Microprobe Facility: Recent Applications in Archaeology," Nuclear Instruments and Methods in Physics Research B30 (1988): 447.

[15]M. Ogawa et al., "A Microprobe System with a Compact Electrostatic Lens," Nuclear Instruments and Methods in Physics Research A239 (1985): 456.

[16]W.M. Augustyniak, et al., "A Miniature Electrostatic Lens for Forming MeV Millibeams," Nuclear Instruments and Methods in Physics Research 149 (1978): 670-71.

[17]J. Raisanen, "An External Beam for PIGE Analysis," Nuclear Instruments and Methods in Physics Research B3 (1984): 221.

[18]K.M. Barfoot, J.D. MacArthur, and C. Vargas-Aburto, "Spatial Intensity Profile Characterization for an External Beram from a Proton Microprobe," Nuclear Instruments and Methods in Physics Research 197 (1982): 121.

[19]Data conversion program written with the help of Midshipman First Class David F. Clipsham and Midshipman First Class John Blalock.

[20]E. Clayton, PIXAN: The Lucas Heights PIXE Analysis Computer Package (Menai, New South Wales: Austrailian Atomic Energy Commission, 1986) 1-4.

[21]M.R. Carriker, C.P. Swann, et al., "An Exploratory Study with the Proton Microprobe of the Ontogenetic Distribution of 16 Elements in the Shell of Living Oysters," Marine Biology 69 (1982): 235.

[22]Clayton, 33.

[23]Bretton W. Kent, Making Dead Oysters Talk (Maryland: Maryland Historical Trust, 1988) 3,13.